Food Research International 107 (2018) 337–345

Contents lists available at ScienceDirect

Food Research International

journal homepage: www.elsevier.com/locate/foodres

Development of LLDPE based active nanocomposite films with nanoclays impregnated with volatile compounds

Fatih Tornuk[a,*], Osman Sagdic[a], Mehmet Hancer[b], Hasan Yetim[c]

[a] Yildiz Technical University, Chemical and Metallurgical Engineering Faculty, Food Engineering Department, Davutpasa Campus, 34210 Istanbul, Turkey
[b] Mugla Sitki Kocman University, Engineering Faculty, Metallurgical and Materials Engineering Department, 48000 Mugla, Turkey
[c] Gelisim University, Faculty of Fine Arts, Gastronomy and Culinary Arts Department, Istanbul, Turkey

ARTICLE INFO

Keywords:
Montmorillonite
Halloysite
Nanocomposite film
Thymol
Eugenol
Carvacrol

ABSTRACT

In this study, a novel procedure was performed for grafting of nanoclays (montmorillonite (MMT) and halloysite (HNT)) with essential oil constituents (thymol (THY), eugenol (EUG) and carvacrol (CRV)) using Tween 80 as surfactant and then the nanoclay particles were incorporated into LLDPE pellets (5 wt%) to produce active nanocomposite films using a twin screw extruder. The resulting nanocomposite films were analyzed for antimicrobial and antioxidant capacity as well as thickness, mechanical, color, barrier, thermal properties and surface morphology and molecular composition. Release of the active compounds from the films at the refrigerated and room temperature conditions were also tested. The results showed that the films had strong in vitro antibacterial activity against pathogenic bacteria (*Salmonella* Typhimurium, *Escherichia coli* O157:H7, *Listeria monocytogenes*, *Staphylococcus aureus* and *Bacillus cereus*) while their effect against lactic acid bacteria (*Lactobacillus rhamnosus* and *Lb. casei*) was limited. The lowest and highest DPPH scavenging ability levels were 65.59% and % 87.92, belonged to THY-MMT and EUG-MMT, respectively. Release of active compounds at 24 °C was much more rapid than at 4 °C. CRV-HNT and THY-HNT provided slower release than the other films. SEM results showed that nanoclays were uniformly dispersed in the polymer matrix with exceptional agglomerates. Incorporation of the active nanoclays significantly ($P > 0.05$) improved tensile strength and elongation of the films. The results confirmed that LLDPE based active nanocomposite films could be successfully produced due to its good interaction with MMT and HNT, activated with THY, EUG and CRV.

1. Introduction

Food packaging is one of the major driving forces of food industry that is consistently gaining new concepts depending on consumer demands. Active packaging is defined as the incorporation of certain additives into packaging materials or into packaging containers in order to maintain/extend shelf life of packaged foods (Day, 2001). Antimicrobial packaging is a form of active packaging which can inactivate/inhibit undesirable microorganisms that may be present in the packaged food (Appendini & Hotchkiss, 2002). As a result of several reasons such as globalization and long transportation periods, increasing consumer demand for fresh and minimally processed foods, strict regulations related to food safety etc., antimicrobial food packaging has gained importance in recent years.

Antimicrobial agents can be applied in the packaging with different ways. Incorporation of antimicrobial agents directly into polymers is one of the most common types of antimicrobial packaging and has several commercial applications. However, direct incorporation of antimicrobials into polymers has some drawbacks such as immiscibility of polymer and antimicrobial because of their hydrophobicity/hydrophilicity and rapid depletion of antimicrobials thereby short period antimicrobial effect (Appendini & Hotchkiss, 2002).

Nanotechnology presents outstanding opportunity in food technology area. Food packaging is one of the major applications of a nanotechnology with the economic magnitude of 4.13 billion USD in 2008 (Mihindukulasuriya & Lim, 2014). Nano-scale fillers such as nanoclays with different geometries has been demonstrated to improve material properties such as mechanical and barrier properties of bio-based and synthetic polymers (Abdollahi, Rezaei, & Farzi, 2012). Nanoclays are characterized with their high surface area giving them high surface activity. Montmorillonite (MMT) and halloysite (HNT) are nanoclays with platelet and tubular structure, respectively. Both clays have been extensively investigated in food packaging applications as nanofillers and carriers of active compounds. In this study, those nanoclays were grafted with active volatile compounds, namely thymol (THY), eugenol (EUG) and carvacrol (CRV) using a novel way of impregnation to

* Corresponding author at: Yildiz Technical University, Chemical and Metallurgical Engineering Faculty, Food Engineering Department, 34210 Esenler, Istanbul, Turkey.
E-mail address: ftornuk@yildiz.edu.tr (F. Tornuk).

https://doi.org/10.1016/j.foodres.2018.02.036
Received 28 August 2017; Received in revised form 9 February 2018; Accepted 13 February 2018
Available online 21 February 2018
0963-9969/

produce active clay nanoparticles. Then linear low density polyethylene (LLDPE) based films were produced by incorporating with the active nanoclays using blown extrusion method. Therefore, this study was conducted to make characterization of the resulting active nanocomposite films impregnated with different active volatile compounds in terms of a series of characteristic properties.

2. Materials and methods

2.1. Film preparation

Linear low-density polyethylene (LLDPE, melt flow index 2000 g/10 min, density 0.918 g/cm^3 at 23 °C, crystal melting point: 121 °C) was provided from Lotrene (Qatofin Company Ltd., Doha, Qatar). Na^+ montmorillonite, (MMT, surface area 250 m^2/g), halloysite, (HNT, surface area 64 m^2/g, 30–70 nm × 1–3 mm nanotube), thymol (THY, 98% purity, vapor pressure 1 mm Hg at 64 °C) and carvacrol (CRV 98% purity) were purchased from Sigma (Germany). Eugenol (EUG, 99% purity) and nonionic Tween 80 (mol wt ~1310) was purchased from Merck (Germany).

Film manufacture procedures were specified in our previous paper (Tornuk, Hancer, Sagdic, & Yetim, 2015). Prior to film preparation, active compounds namely THY, CRV and EUG were impregnated to the nanoclays. For this purpose, 3 mL of active compound and Tween 80 were mixed in a beaker at room temperature. Distilled water (100 mL) was slowly incorporated with the active compound/surfactant mixture under continuous mixing for ~10 min. Then the nanoclay (3 g) was added into the mixture and mixing was proceeded for 3 h at ambient conditions. The precipitate was obtained by the centrifugation of the suspension at 5000 rpm for 5 min and dried at room temperature for 48 h. The nanoclay particles loaded with the active compounds were obtained by milling the dried nanoparticles using a ball mill (Fritsch™ Pulverisette 7 Premium Line, Germany).

Melt intercalation method was used for production of LLDPE based active nanocomposite films. A twin-screw extruder (L/D = 35, D = 16 mm, Gulnar Machines, Istanbul, Turkey) and a temperature profile of 40, 175, 180, 175 and 180 °C was employed for film production. Extrusion parameters such as feeding rate, temperature profile was optimized by preliminary works. The clay nanoparticles were incorporated with the LLDPE pellets (5 wt%) from the same feeding port. The active nanocomposite films were prepared as stated in Table 1. Control sample was prepared without incorporation of the active clay nanoparticles. In our preliminary studies, due to the poor antimicrobial/antioxidant activity of EUG grafted HNT nanoparticles, it was not used in nanocomposite film production as a nanofiller and thereby not listed in Table 1.

2.2. Scanning electron microscopy

Surface morphologies of the LLDPE based active nanocomposite films were analyzed by SEM (SEM LEO 440 Stereoscan). At least 10 images were obtained.

Table 1
Active compound grafted nanocomposite film samples prepared by melt extrusion method.

Sample No	Film ID	Film information
1	Control	Neat LLDPE film
2	CRV-MMT	LLDPE film reinforced with carvacrol grafted montmorillonite
3	CRV-HNT	LLDPE film reinforced with carvacrol grafted halloysite
4	EUG-MMT	LLDPE film reinforced with eugenol grafted montmorillonite
5	THY-MMT	LLDPE film reinforced with thymol grafted montmorillonite
6	THY-HNT	LLDPE film reinforced with thymol grafted halloysite

2.3. Fourier transform infrared (FTIR) spectroscopy

In order to make molecular characterization of the active nanocomposite films reinforced with the nanoclays grafted with THY, EUG or CRV, their FTIR spectra was analyzed by a FTIR tool (Perkin Elmer Spectrum 400, Perkin Elmer Instruments, USA). Measurements were performed at 450–4000 cm^{-1} wavelength (Siripatrawan & Harte, 2010).

2.4. Thermal properties

Weight loss of the film samples during heating was analyzed by thermogravimetric analysis (TGA). In this process, the film samples were placed into the balance system and heated from 50 °C to 600 °C with a heating rate of 20 °C/min. The weight loss was measured as a function of temperature (Morawiec et al., 2005).

Thermal behavior of the active nanocomposite films were determined by differential scanning calorimetry (DSC, Model DSC-7, Perkin Elmer Instruments, USA). Five to ten milligrams of the film sample was placed into aluminum pans and heated from −10 °C to 160 °C. Melting temperature (T_m) and melting enthalpy (ΔH) were obtained. Crystallization level was calculated by the proportion between ΔH levels of the sample and 100% crystalline polyethylene (293 J/g). T_{95} and T_{50} values were also obtained in order to give information about thermal degradation of the samples.

2.5. Optical properties

Color properties (L^*, a^* and b^* values) of the LLDPE based active nanocomposite films were analyzed by a Hunter colorimeter (Lovibond RT Series Reflectance Tintometer, UK) (Rhim, Hong, Park, & Ng, 2006). Total color difference (ΔE) was calculated with the following formula:

$$\Delta E = (\Delta L^2 + \Delta a^2 + \Delta b^2)^{0.5} \quad (1)$$

where $\Delta L = L_{standard} - L_{sample}$, $\Delta a = a_{standard} - a_{sample}$ and $\Delta b = b_{standard} - b_{sample}$ while standard values of the white plate were $L = 94.98$, $a = -1.04$ and $b = 0.55$.

Opacity values (%) of the film samples were determined by reflectance measurements according to Hunter lab method (Casariego et al., 2009).

2.6. Film thickness

Thickness of the active nanocomposite films reinforced with was measured using a digital micrometer (Fowler Digitrix Mark 2, Chicago, USA).

2.7. Oxygen permeability

Oxygen permeability (OP) of the active nanocomposite films was measured under controlled conditions (0% RH and 23 °C) based on the standard method of ASTM (2010) using an OxTran ST-2/21 modular system (Mocon Inc., Minneapolis, USA). The results were obtained as cc/m^2·24 h taking account of the thickness values of the film samples.

2.8. Mechanical properties

Tensile strength (TS) and elongation at break (EB) values of the LLDPE based nanocomposite films were determined according to the standard method of ASTM (2012) using a texture analyzer (TA.XT Plus Stable Micro Systems, Surrey, UK) with a load cell of 5 kg. The film samples were cut in rectangular shapes (10 cm × 2 cm). The initial distance between the grips and crosshead speed were set to 50 mm and 4 mm/s, respectively. At least five replications were performed in order

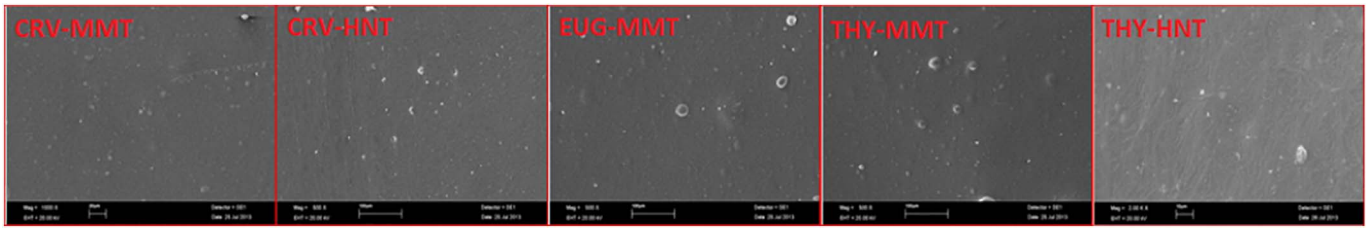

Fig. 1. SEM images of the active compound grafted nanocomposite films.

to determine the TS and EB.

2.9. Quantification of active compounds

Amounts of THY, EUG and CRV in the active nanocomposite films and their decrease during storage at 4 and 24 °C for 40 days were analyzed by gas chromatography (GC, Agilent 6890, USA) equipped with flame ionization detector and fused capillary column (DB-5, 30 m × 0.25 mm i.d., film thickness 0.25 mm; J&W Scientific, USA) as explained by Suppakul, Miltz, Sonneveld, and Bigger (2006). Following incorporation of 4 mL of methanol into 2 g of the film sample and keeping at room temperature for 24 h, the methanolic extract was injected into the GC. Analysis conditions followed were: initial column temperature, 80 °C; 5 °C/min to 180 °C; held for 5 min before sampling; injector temperature, 250 °C; split ratio, 1:100; FID detector temperature, 300 °C; carrier gas, hydrogen; injection level, 0.1 μL.

In order to determine the effect of the nanoclays on active compound loss during melt extrusion, control LLDPE films were produced with the addition of CRV, THY or EUG (without nanoclay) at the same extrusion conditions. The results were compared with those of the active nanocomposite films.

2.10. Antimicrobial activity

Antimicrobial activity of the active nanocomposite films was determined by shake flask test as described by Appendini and Hotchkiss (2002) and Sothornvit, Rhim, and Hong (2009) with some modifications. Five pathogenic and two lactic acid bacterial (LAB) strains including *Staphylococcus aureus* ATCC 25923, *Listeria monocytogenes* ATCC 19118, *Escherichia coli* O157:H7 ATCC 33150, *Bacillus cereus* FMC19, *Lactobacillus casei* and *Lb. rhamnosus* were tested. Cryopreserved LABs and pathogenic strains were twice activated in MRS (Merck, Germany) and Nutrient Broth (Merck, Germany), respectively and inoculated into sterilized buffer solutions (100 mL, pH = 7) prepared with KH_2PO_4 (Merck, Germany) and Na_2HPO_4 (Merck, Germany) at a targeted level of ~10^6 cfu/mL. Film samples with a total surface area of 25 cm^2 were cut into small pieces and put into the flasks. Then the flasks were incubated at 37 °C for 24 h. Numbers of the bacteria were determined after the incubation with spread plate method and expressed as log cfu/mL.

In order to characterize the antimicrobial efficiency of the active nanocomposite films, growth inhibition levels (GILs, %) of the bacteria were calculated according to following equation:

$$GIL = \frac{P_C - P_S}{P_C} \times 100 \quad (2)$$

where *Pc* and *Pc* are populations of the control and the sample after the incubation, respectively.

2.11. Antioxidant activity (AOA)

DPPH radical scavenging activities of the LLDPE based active nanocomposite films were determined based on the method described by (Byun, Kim, & Whiteside, 2010). For this purpose, 0.1 g of the film sample was cut into small pieces and incorporated with 2 mL of methanol in a test tube. The mixture was kept at room temperature after vortexed for 3 min. Vortex homogenization was repeated and it was centrifuged at 2300 rpm for 10 min. After centrifugation, 500 μL of the supernatant was incorporated with 2 mL of 0.06 mM DPPH solution (in methanol) while the sample was 0.12 mM DPPH solution was used as control. The resulting mixture was vortexed for 1 min and kept for 30 min in dark. The absorbance was measured at 517 nm using a spectrophotometer (Shimadzu UV–visible 1700, Tokyo, Japan). The AOA (%) was determined using the following equation:

$$AOA = \left(1 - \frac{A_S}{A_C}\right) \times 100 \quad (3)$$

where A_s and A_c are absorbance values of the sample and the control, respectively.

2.12. Statistical analysis

In this study, a Windows based statistical analysis software (SAS 8.2, SAS Institute, Cary, North Carolina, USA) was used to perform the two-way analysis of variance (ANOVA). Differences between the data were evaluated by using Duncan's multiple comparison test at a significance level of 95%. All the analyses were carried out in triplicate.

3. Results and discussion

3.1. SEM

Morphological properties and distribution of active clay nanoparticles in the film matrix were analyzed by SEM. In SEM micrographs (Fig. 1), the nanoclay particles are seen as white dots. The micrographs indicated that active compound impregnated nanoclays showed a good distribution in the LLDPE film matrix with several agglomerates while the nanoclays grafted with the active compounds incorporated into the CRV-MMT and THY-HNT samples exhibited better dispersion. In this study, a 5 wt% of active nanoclay concentration was selected since higher (7.5 wt%) nanoclay concentration formed tactoids and clusters. Suitable filler concentration should be selected in order to provide the uniform dispersion of the filler and to prevent the presence of agglomeration in film matrix without breakage of the film and reduction its quality (Cayer-Barrioz et al., 2006; Ščetar, Siročić, Hrnjak-Murgić, & Galić, 2013). Extrusion processing variables such as feeding rate, screw speed and screw profile are also important parameters for achievement of a good polymer/filler interaction (Da Silva, Canto, & Visconti, 2010).

3.2. FTIR

Molecular characterization of the active nanocomposite films were analyzed by FTIR as seen in Fig. 2. Incorporation of the nanoclays into the polymer matrix caused variations in the FTIR profiles of the films. Vibrations at 450–500 cm^{-1} and 1000–1100 cm^{-1} wavelength which were absent in the neat LLDPE film were observed at the active nanocomposite films (Fig. 7). The FTIR spectra belonging to LLDPE film produced in this research was similar to that of previous reports (Morlat-Therias et al., 2008; Zan, Fa, & Wang, 2006). The broad peaks at 2800–2900 cm^{-1} represent that CH_2═CH_2 (ethylene) bonds of

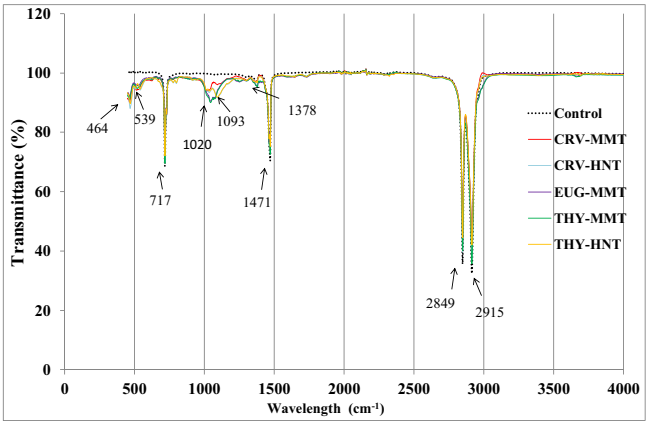

Fig. 2. FTIR spectra of the active compound grafted nanocomposite films.

polyethylene were not degraded at extrusion conditions for both neat LLDPE film and active nanocomposite films (García, Hoyos, Guzmán, & Tiemblo, 2009). The vibrations at 1000–1100 cm^{-1} correspond to the energy absorbed by Si—O bonds while the peaks observed at 450–550 cm^{-1} are caused by vibration of Si—O—Si and Si—O—Al groups (Durmuş, Woo, Kaşgöz, Macosko, & Tsapatsis, 2007), which demonstrates the presence of nanoclays MMT or HNT in the film samples. The slight vibrations seen at 3600–3700 cm^{-1} are also typical to the nanoclays (Krepker et al., 2018). Weak peaks between 750 and 800 cm^{-1} wavelengths which belong to THY-MMT and THY-HNT are associated with ring vibrations of thymol (Sanchez-Garcia, Ocio, Gimenez, & Lagaron, 2008) while carvacrol had characteristic peaks resulting from the vibrations of C—H bonds of aromatic rings at 900–650 cm^{-1} region (Krepker et al., 2018).

3.3. Thermal properties

Thermogravimetric analysis (TGA) gives information about thermal behavior of film materials at elevated temperatures. As seen in TGA profiles of the nanocomposite films in Fig. 3, the film samples exhibited similar behaviors up to 420 °C at which thermal degradation started. One step decomposition was observed in the all samples indicating the decomposition of the polymer. Incorporation of active nanoclays into the LDPE matrix remarkably increased T_{95} (temperature which 5% weight loss occurred) values, as can be seen in Table 2. The highest and lowest T_{95} values were 449.30 °C and 400.65 °C (which were belonged to CRV-HNT and THY-MMT), respectively. In all cases, incorporation of HNT nanoclay gave higher T_{95} values. T_{50} (temperature which 50% weight loss occurred) values which were also given in Table 2 ranged from 481.64 to 491.45 °C. The results were in accordance with the findings of Hemati and Garmabi (2011) who reported that T_{50} values of LDPE/LLDPE blends and their nanocomposites were between 474 and 485 °C in the nitrogen atmosphere.

Table 2
Thermal properties of the active compound grafted nanocomposite films as measured by DSC and TGA analysis.

Sample	ΔH (J/g)	T_m (°C)	χ (%)	T_{50} (°C)	T_{95} (°C)
Control	75.22	109.09	25.67	486.70	427.95
CRV-MMT	56.65	117.41	19.33	489.13	440.73
CRV-HNT	41.55	117.87	14.18	491.45	449.30
EUG-MMT	55.36	117.75	18.89	485.84	430.78
THY-MMT	68.35	116.92	23.33	481.64	400.65
THY-HNT	54.37	117.38	18.56	488.42	442.73

ΔH: Total enthalpy; T_m: Melting temperature; χ: Crystallization level; T_{50} and T_{95}: Temperatures which 50% and 5% weight loss occurred, respectively.

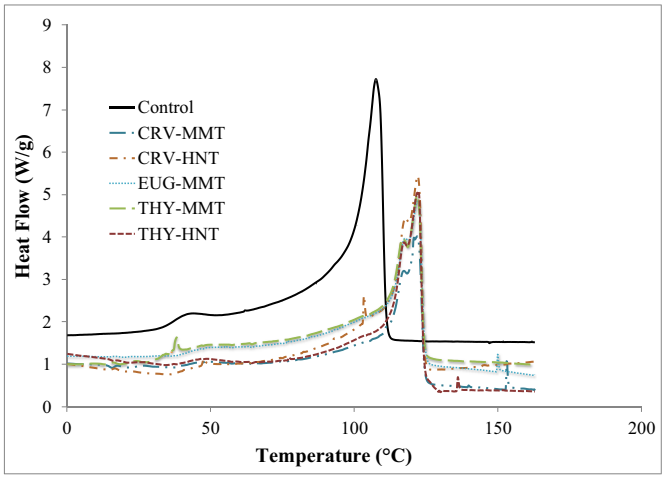

Fig. 4. DSC thermograms of the active compound grafted nanocomposite films.

Fig. 4 shows DSC thermograms of the LLDPE based active nanocomposite films. It was clear that melting point of the neat LLDPE film was lower than those of the nanocomposite films. In addition, two endothermic peaks were observed in the film samples incorporated with active nanoclays while the LLDPE film exhibited one endothermic peak. Other thermal characteristics of the film samples were given in Table 2. Incorporation of the nanoclays impregnated with EUG, THY or CRV into the LLDPE polymer decreased its crystallinity from 25.67% to the levels ranging from 14.18% to 23.33%. The film samples containing HNT (CRV-HNT and THY-HNT) had lower crystallinity values than those containing MMT (CRV-MMT and THY-MMT). On the other hand, a notable effect of active compounds on degree of crystallinity of the

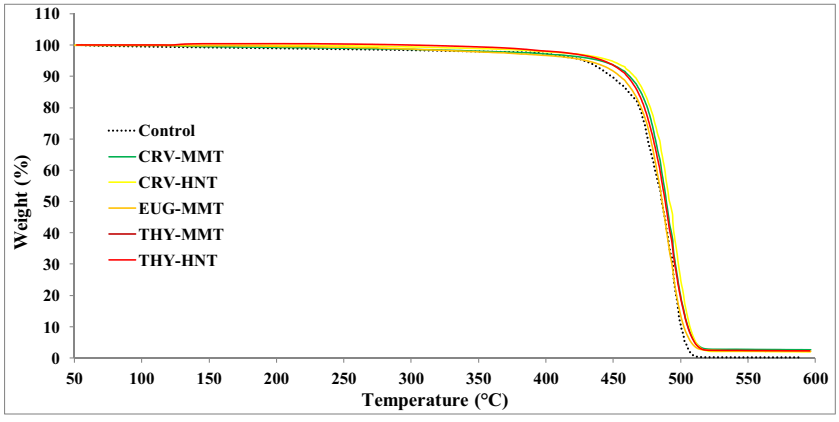

Fig. 3. TGA profiles of the active compound grafted nanocomposite films.

Table 3
Optical properties of the active compound grafted nanocomposite films.

Sample	L^*	a^*	b^*	ΔE	Opacity (%)
Control	93.92 ± 0.06^{a}	−1.15 ± 0.02^{cd}	0.34 ± 0.02^{d}	1.09	4.01 ± 0.29^{a}
CRV-MMT	93.08 ± 0.18^{bc}	−1.16 ± 0.02^{d}	1.23 ± 0.10^{c}	2.02	4.44 ± 0.21^{a}
CRV-HNT	92.80 ± 0.47^{bc}	−1.09 ± 0.03^{ab}	1.73 ± 0.17^{ab}	2.47	4.51 ± 0.28^{a}
EUG-MMT	93.18 ± 0.25^{b}	−1.14 ± 0.05^{bcd}	1.46 ± 0.20^{bc}	2.02	4.41 ± 0.40^{a}
THY-MMT	91.95 ± 0.18^{d}	−1.10 ± 0.02^{abc}	1.47 ± 0.13^{bc}	3.17	4.21 ± 0.11^{a}
THY-HNT	92.58 ± 0.32^{c}	−1.08 ± 0.03^{a}	1.76 ± 0.20^{a}	2.69	4.65 ± 0.05^{a}

ΔE: Total color difference; $^{a–d}$: The same uppercase letters within the same column for each sample show that the results are not statistically significantly different ($P > 0.05$).

active nanocomposite films was not observed. Decrease in crystallinity by reinforcement of LLDPE with the nanoclays can be explained by the good interaction between the nanofillers and LLDPE which significantly hindered the chain mobility of the polymer (Durmuş et al., 2007; Kuila et al., 2012). Similarly, Dadbin, Noferesti, and Frounchi (2008) also reported that addition of organoclay led to increase in T_m and decrease in the crystallinity level of LDPE/LLDPE films while Golebiewski, Rozanski, Dzwonkowski, and Galeski (2008) found that crystallinity degree of LDPE based films containing different nanoclays ranged from 47.1% to 49.4%. Melting temperatures (T_m) of the active nanocomposite films varied from 116.92 °C to 117.87 °C which were higher than that of the neat LLDPE film (109.09 °C). Melting behaviors of the active nanocomposite films were also correlated with degree of crystallinity as well as chain mobility, which was also specified by Durmuş et al. (2007) and Kuila et al. (2012).

3.4. Optical properties

Color values, total color difference (ΔE) and opacity of the active nanocomposite films produced in this study are presented in Table 3. Slight but significant ($P < 0.05$) changes were observed in L^*, a^* and b^* values of the films by the addition of clay nanoparticles into the LLDPE film. ΔE values ranged from 1.09 to 3.17 which were belonged to the neat LLDPE film and THY-MMT, respectively. The differences between opacity values of the films were not significant ($P > 0.05$). Similarly, a decrease in L^* and a^* values with addition of nanoclays has already been reported in the literature (Park et al., 2002; Sothornvit et al., 2009). Sothornvit et al. (2009) found that whey protein isolate based films supplemented with Cloisite Na+, Cloisite 20A and Cloisite 30B had lower in L^* and a^* but higher b^* and ΔE values as compared to the control sample. Such a result was attributed to the high hydrophobicity of the nanoclays and their good dispersion in the polymer matrix (Park et al., 2002). Similar results were also reported by Rhim (2011) and Farahnaky, Dadfar, and Shahbazi (2014).

3.5. Film thickness

Film thickness of the active nanocomposite films varied from 20 μm to 45 μm as shown in Table 4. LLDPE film had the lowest ($P < 0.05$) thickness while no statistical difference ($P > 0.05$) was observed between the thickness values of the film samples reinforced with the active nanoclays. The results were in accordance with the previous literature (Golebiewski et al., 2008; Shah, Krishnaswamy, Takahashi, & Paul, 2006; Zan et al., 2006). In another study, mean thickness of LDPE/MMT films was around 50–60 μm (Arunvisut, Phummanee, & Somwangthanaroj, 2007) which was higher than our findings.

3.6. Oxygen permeability

As seen in Table 4, oxygen permeability values were significantly ($P < 0.05$) influenced from nanoclay incorporation and nanoclay type (MMT or HNT). As expected, active nanoclay incorporation significantly ($P < 0.05$) decreased the oxygen permeability of the films. Especially, HNT incorporated films provided lower ($P < 0.05$) permeability values, indicating that effect of HNT was better than that of MMT. Similar findings were also noted by Pereira de Abreu, Paseiro Losada, Angulo, and Cruz (2007) who found that lower oxygen permeability levels were obtained by addition of Cloisite 15A nanoclay into LDPE and polypropylene based films. Memiş, Tornuk, Bozkurt, and Durak (2017) reported that oxygen permeability of fenugreek seed gum based films decreased depending on the increasing nanoclay content.

The theory suggested by Nielsen (1967) to explain the improvement of barrier properties of polymer/clay nanocomposites is the most widely accepted one. According to this theory, the permeant is forced to travel through a longer path to permeate because of the tortuous structure of the clay. Decrease in oxygen permeability by addition of the nanoclays also indicates the good orientation (intercalation/exfoliation) of the clay.

3.7. Mechanical properties

Mechanical properties namely elongation at break (EB) and tensile strength (TS) values of the nanocomposite film samples were seen in Table 4. Significant differences ($P < 0.05$) in TS and EB values were observed by nanoclay incorporation into the LLDPE based film. For example, TS values of CRV-MMT and EUG-MMT were higher ($P < 0.05$) than the other film samples while incorporation of all the active clay nanoparticles increased the EB values significantly ($P < 0.05$). Two types of clays derived from MMT was found to develop mechanical properties of LLDPE based films (Hotta & Paul, 2004). Similar results were also reported by Kanmani and Rhim (2014), Müller, Laurindo, and Yamashita (2011) and Almasi, Ghanbarzadeh,

Table 4
Thickness, oxygen permeability (OP) and some mechanical properties of the active compound grafted nanocomposite films.

Sample	Thickness (μm)	OP (cc/m^2·24 h)	TS (MPa)	EB (%)
Control	20.00 ± 0.00^{b}	11,035.23 ± 1315.68^{a}	4.69 ± 0.29^{c}	334.48 ± 16.42^{c}
CRV-MMT	37.50 ± 3.54^{ab}	6508.87 ± 1483.58^{bc}	7.90 ± 0.42^{a}	485.67 ± 43.26^{a}
CRV-HNT	45.00 ± 0.00^{a}	6147.64 ± 665.24^{bc}	4.73 ± 0.28^{c}	461.78 ± 11.21^{a}
EUG-MMT	30.00 ± 7.07^{ab}	8852.76 ± 1407.42^{ba}	7.31 ± 0.23^{b}	481.81 ± 25.99^{a}
THY-MMT	35.00 ± 7.07^{ab}	9219.71 ± 1572.83^{ba}	4.49 ± 0.24^{c}	407.18 ± 24.30^{b}
THY-HNT	37.50 ± 3.54^{ab}	4812.69 ± 414.30^{c}	4.89 ± 0.29^{c}	384.89 ± 8.81^{b}

OP: Oxygen permeability; TS: Tensile strength; EB: Elongation at break; $^{a-d}$: The same uppercase letters within the same column for each sample show that the results are not statistically significantly different ($P > 0.05$).

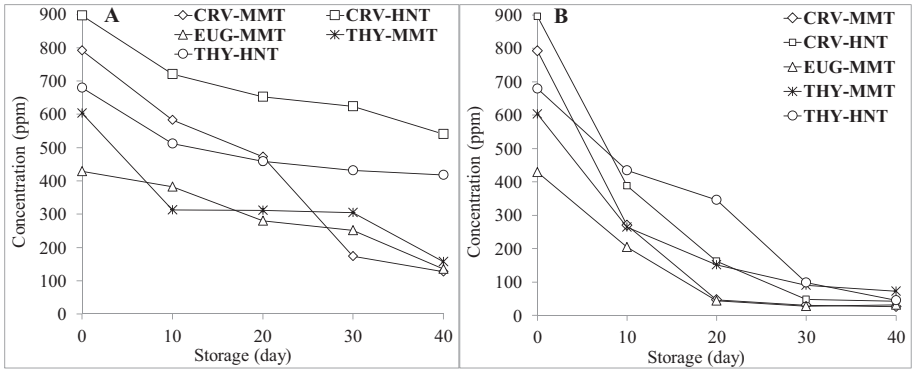

Fig. 5. Change of the active compounds in the active nanocomposite films during storage at 4 °C (A) or 24 °C (B).

and Entezami (2010). Considering the overall mechanical properties, it was concluded that improvement in mechanical properties was attributed to not only nanoclay type and dispersion but also crystallinity levels of the active nanocomposite films as given in Table 2. In general, decrease in crystallinity caused increase in EB values of the film samples while TS values were not directly correlated with degree of crystallinity. A similar relationship between EB and crystallinity was found by Memiş et al. (2017) who reported that nanoclay (HNT and MMT) incorporation increased crystallinity but decreased EB of fenugreek gum based nanocomposite films. Increase in EB with the addition of nanofillers into film matrix was also reported by Kontou and Niaounakis (2006).

3.8. Quantity of the active compounds

Residual quantities of the active compounds impregnated into the active nanocomposite films were analyzed during storage at refrigerated and ambient conditions for 40 days. As can be seen in Fig. 5, initial concentrations of the active compounds were between 429.18 ppm (EUG-MMT) and 896.22 (CRV-HNT), indicating that EUG was the most susceptible compound against film extrusion conditions. As expected, release of the active compounds at 24 °C were more rapid than at 4 °C. A rapid decrease was observed in active compound levels of the films at the first 10 days of the storage at 24 °C while the levels declined below 100 ppm after 40 days (Fig. 5B). In the meanwhile, the highest ($P < 0.05$) active compound levels were observed at CRV-HNT (541.07 ppm) and THY-HNT (417.66 ppm) at the end of the storage at 4 °C (Fig. 5A). Considering the effects of nanoclay types on the release of active compounds from the films, active compound levels of the film samples produced with HNT had higher concentrations than those of the films containing MMT during the storage at both temperatures (Fig. 6A and B). This indicates that HNT nanoclay provided a slower release of the active compounds as compared to MMT.

As known, extremely high temperatures (generally higher than 150 °C) above melting point of plastics is needed for the film extrusion processing. Since volatile compounds such as essential oils or their constituents are regarded as heat sensitive materials (Appendini & Hotchkiss, 2002), they are likely exposed to evaporation or degradation during the film production by extrusion (Suppakul et al., 2006). In our preliminary studies, higher levels of loss of the active compounds occurred when neat LLDPE was extruded at the same conditions after compounding with CRV, EUG or THY. This shows that nanoclays enabled protective effect on the active compounds against evaporation during film production and/or there was a good interaction between the active compounds and the nanoclays. This finding was also noted by Persico et al. (2009).

3.9. Antimicrobial activity

Antimicrobial activity of the active nanocomposite films was tested with shake flask method against some foodborne pathogens and lactic acid bacteria (LAB) and the results were shown in Tables 5 and 6, respectively. In general, it was clear that the pathogenic bacteria were more susceptible to the film samples than LAB. Among the pathogens, *B. cereus* and *S. aureus* were the most susceptible and the most resistant bacteria during the treatment period, respectively. All the active nanocomposite film samples provided significant ($P < 0.05$) reductions in the microbial numbers. THY-MMT achieved complete elimination of *B. cereus*, *E. coli* O157:H7, *S.* Typhimurium and *L. monocytogenes* while effect of EUG-MMT on those pathogens were limited (Table 5).

On the other hand, as seen in Table 6, limited influence of the active nanocomposite films was observed on *Lb. rhamnosus* and *Lb. casei*. Although statistically significant ($P < 0.05$) reductions occurred compared to the control sample, the growth inhibition levels (GILs) did not exceed 17.99% and 15.17% for *Lb. rhamnosus* and *Lb. casei*, respectively.

Agar diffusion is the most common method to determine antimicrobial effects of active packaging films. However, it is relatively easy to conduct but the results are generally qualitative (Suppakul, 2012). Therefore in this study, buffered solution at pH 7.0 was used for testing the antibacterial activity. This method has been used by several other researchers (Fajardo, Balaguer, Gomez-Estaca, Gavara, & Hernandez-Munoz, 2014; Zivanovic, Li, Davidson, & Kit, 2007). In this method, the ratio between total film surface area and liquid volume is the most important parameter. This test gives opportunity to test real food conditions (Appendini & Hotchkiss, 2002).

Antibacterial activity of films obtained by incorporation of nanoclays and volatile oils/compounds were tested by several researchers. Persico et al. (2009) reported that LDPE films reinforced with 10% CRV and 5% organomodified nanoclay showed antibacterial activity against *B. thermosphacta*, *L. innocua* and *Carynobacterium*. Lim, Jang, and Song (2010) tested antibacterial activity of *Gelidium corneum* based films containing two types of nanoclays as well as THY and grape seed extract at different concentrations against *E. coli* O157:H7 and *L. monocytogenes*. Shemesh et al. (2015) found that LDPE/(clay/CRV) films exhibited superior and prolonged antibacterial activity against *E. coli* and *Listeria innocua*, while polymer compounded with pure CRV lost the antibacterial properties within days. The films also showed good antifungal activity against *Alternaria alternata*.

3.10. Antioxidant activity (AOA)

In this study, in order to determine the ability of active nanocomposite films to control oxidation in foods, their DPPH radical scavenging activities were determined. As seen in Fig. 7, the film samples showed significant AOA with the levels ranging from 65.59% to 87.92%, as measured by DPPH radical inhibition. EUG-MMT showed the highest ($P < 0.05$) AOA followed by THY-HNT while neat LLDPE film (control) did not show any radical scavenging activity. This result indicates that antioxidant properties of the nanocomposite films are

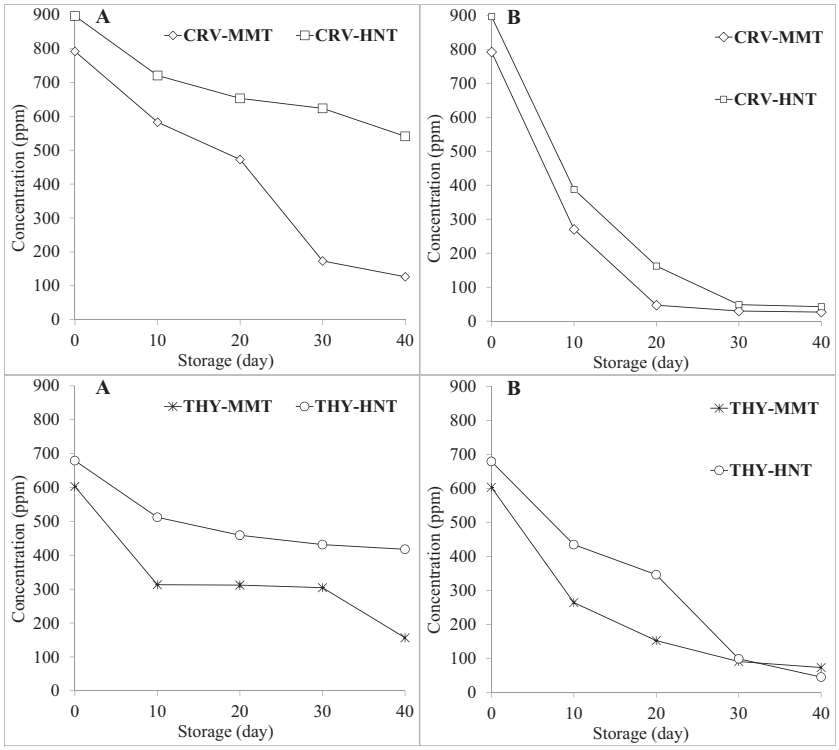

Fig. 6. Effect of the nanoclays on concentrations of the active compounds in the active nanocomposite films during storage at 4 °C (A) or 24 °C (B).

Table 5
Antimicrobial properties of the active compound grafted nanocomposite films against foodborne pathogens.

Film sample	*Escherichia coli* O157:H7		*Listeria monocytogenes*		*Salmonella* Typhimurium		*Staphylococcus aureus*		*Bacillus cereus*	
	Log cfu/mL	GIL (%)	Log cfu/mL	GIL (%)	Log cfu/mL	GIL (%)	Log cfu/mL	GIL (%)	Log cfu/mL	GIL (%)
Control	7.70 ± 0.03^{a}	–	7.15 ± 0.17^{a}	–	7.34 ± 0.03^{a}	–	7.59 ± 0.13^{a}	–	6.22 ± 0.17^{a}	–
CRV-MMT	< 1.00^{d}	100.00	3.69 ± 0.10^{d}	48.39	6.15 ± 0.06^{c}	16.21	6.90 ± 0.11^{b}	9.09	3.75 ± 0.08^{c}	39.71
CRV-HNT	4.85 ± 0.09^{c}	37.01	5.04 ± 0.02^{b}	29.51	3.37 ± 0.23^{e}	54.09	5.50 ± 0.12^{c}	27.54	< 1.00^{d}	100.00
EUG-MMT	7.34 ± 0.07^{b}	4.68	4.54 ± 0.31^{c}	36.50	6.73 ± 0.08^{b}	8.31	6.87 ± 0.04^{b}	9.49	6.01 ± 0.10^{b}	3.38
THY-MMT	< 1.00^{d}	100.00	< 1.00^{e}	100.00	< 1.00^{f}	100.00	5.23 ± 0.04^{d}	31.09	< 1.00^{d}	100.00
THY-HNT	< 1.00^{d}	100.00	< 1.00^{e}	100.00	4.75 ± 0.11^{d}	35.29	5.29 ± 0.05^{d}	30.30	< 1.00^{d}	100.00

GIL: Growth inhibition level; $^{a–e}$: The same uppercase letters within the same column for each sample show that the results are not statistically significantly different ($P > 0.05$).

Table 6
Antimicrobial properties of the active compound grafted nanocomposite films against lactic acid bacteria.

Sample	*Lactobacillus rhamnosus*		*Lactobacillus casei*	
	Log cfu/mL	GIL (%)	Log cfu/mL	GIL (%)
Control	7.28 ± 0.08^{a}	–	7.78 ± 0.06^{a}	–
CRV-MMT	5.97 ± 0.37^{c}	17.99	6.60 ± 0.20^{b}	15.17
CRV-HNT	6.41 ± 0.28^{cb}	11.95	6.73 ± 0.20^{b}	13.50
EUG-MMT	6.64 ± 0.07^{b}	8.79	6.83 ± 0.19^{b}	12.21
THY-MMT	6.34 ± 0.08^{cb}	12.91	6.67 ± 0.10^{b}	14.27
THY-HNT	6.12 ± 0.15^{c}	15.93	5.29 ± 0.05^{c}	32.01

GIL: Growth inhibition level; $^{a–c}$: The same uppercase letters within the same line for each sample show that the results are not statistically significantly different ($P > 0.05$).

influenced from the presence of phenolic compounds, THY, CRV and EUG. Radical scavenging abilities of polymeric films containing phenolic compounds have also been reported in the literature (M. López-Mata et al., 2013; M. A. López-Mata et al., 2017; Ramos, Jiménez, Peltzer, & Garrigós, 2014).

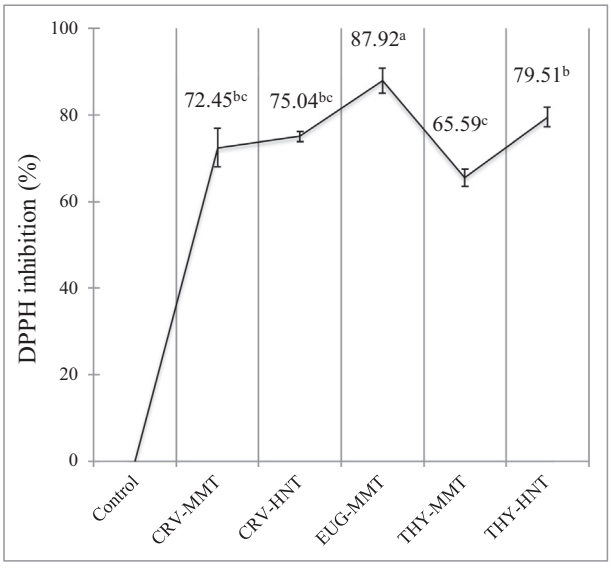

Fig. 7. Antioxidant activity of the active compound grafted nanocomposite films as measured by DPPH radical scavenging ability (%).

4. Conclusion

In this study, THY, EUG and CRV were grafted to MMT and HNT nanoclays with a new method via Tween 80 as surfactant to produce activated clay nanoparticles. Active nanoclays were successfully incorporated into LLDPE based blown films, and the grafting method was effective for protection of active compounds against degradation and evaporation during the film production via extrusion. There was a good interaction between the activated nanoclays and LLDPE as indicated by SEM micrographs. Incorporation of the nanoclays into the polymer matrix caused variations in the FTIR profiles of the films, indicating the interaction between the materials. Weight loss was retarded and melting temperature of LLDPE was increased by active nanoclay incorporation as measured by DSC and TGA analyses while nanoclay addition decreased degree of crystallinity. Active nanoclay incorporation decreased the oxygen permeability of the films, especially HNT incorporated films had lower permeability values than MMT containing samples. The results indicated that the nanocomposite films showed remarkable antimicrobial activity against foodborne pathogenic bacteria with limited efficiency against LAB while antioxidant activity as measured by DPPH radical scavenging was also noticeable. Active nanocomposite films provided controlled (balanced) release of the active compounds. In conclusion, it can be suggested that this method could be used for the grafting nanoclays with volatile essential oils to use in the production of active nanocomposite films for food packaging applications.

Acknowledgement

We would like to thank Erciyes University for providing funds for this project with project number FDK-2013-4235 of the Scientific Research Project Unit of Erciyes University of Turkey.

References

Abdollahi, M., Rezaei, M., & Farzi, G. (2012). A novel active bionanocomposite film incorporating rosemary essential oil and nanoclay into chitosan. *Journal of Food Engineering, 111*(2), 343–350. http://dx.doi.org/10.1016/j.jfoodeng.2012.02.012.

Almasi, H., Ghanbarzadeh, B., & Entezami, A. A. (2010). Physicochemical properties of starch–CMC–nanoclay biodegradable films. *International Journal of Biological Macromolecules, 46*(1), 1–5. http://dx.doi.org/10.1016/j.ijbiomac.2009.10.001.

Appendini, P., & Hotchkiss, J. H. (2002). Review of antimicrobial food packaging. *Innovative Food Science & Emerging Technologies, 3*(2), 113–126. http://dx.doi.org/10.1016/S1466-8564(02)00012-7.

Arunvisut, S., Phummanee, S., & Somwangthanaroj, A. (2007). Effect of clay on mechanical and gas barrier properties of blown film LDPE/clay nanocomposites. *Journal of Applied Polymer Science, 106*(4), 2210–2217. http://dx.doi.org/10.1002/app.26839.

ASTM (2010). *ASTM D3985-05 standard test method for oxygen gas transmission rate through plastic film and sheeting using a coulometric sensor*. West Conshohocken, PA: ASTM Internationalhttp://dx.doi.org/10.1520/D3985-05R10E01.

ASTM (2012). *Standard test method for tensile properties of thin plastic sheeting.* West Conshohocken, PA: ASTM Internationalhttp://dx.doi.org/10.1520/D0882-12.

Byun, Y., Kim, Y. T., & Whiteside, S. (2010). Characterization of an antioxidant polylactic acid (PLA) film prepared with α-tocopherol, BHT and polyethylene glycol using film cast extruder. *Journal of Food Engineering, 100*(2), 239–244. http://dx.doi.org/10.1016/j.jfoodeng.2010.04.005.

Casariego, A., Souza, B. W. S., Cerqueira, M. A., Teixeira, J. A., Cruz, L., Díaz, R., & Vicente, A. A. (2009). Chitosan/clay films' properties as affected by biopolymer and clay micro/nanoparticles' concentrations. *Food Hydrocolloids, 23*(7), 1895–1902. http://dx.doi.org/10.1016/j.foodhyd.2009.02.007.

Cayer-Barrioz, J., Ferry, L., Frihi, D., Cavalier, K., Séguéla, R., & Vigier, G. (2006). Microstructure and mechanical behavior of polyamide 66-precipitated calcium carbonate composites: Influence of the particle surface treatment. *Journal of Applied Polymer Science, 100*(2), 989–999. http://dx.doi.org/10.1002/app.22826.

Da Silva, C., Canto, L., & Visconti, L. (2010). Effect of extrusion processing variables on the polyethylene/clay nanocomposites rheological properties. *Chemistry & Chemical Technology, 4*(1), 61–68.

Dadbin, S., Noferesti, M., & Frounchi, M. (2008). Oxygen barrier LDPE/LLDPE/organoclay nano-composite films for food packaging. *Macromolecular Symposia, 274*(1), 22–27. http://dx.doi.org/10.1002/masy.200851404.

Day, B. (2001). Active packaging-a fresh approach. *The Journal of Brand Technology, 1*(1), 32–41.

Durmuş, A., Woo, M., Kaşgöz, A., Macosko, C. W., & Tsapatsis, M. (2007). Intercalated linear low density polyethylene (LLDPE)/clay nanocomposites prepared with oxidized polyethylene as a new type compatibilizer: Structural, mechanical and barrier properties. *European Polymer Journal, 43*(9), 3737–3749. http://dx.doi.org/10.1016/j.eurpolymj.2007.06.019.

Fajardo, P., Balaguer, M. P., Gomez-Estaca, J., Gavara, R., & Hernandez-Munoz, P. (2014). Chemically modified gliadins as sustained release systems for lysozyme. *Food Hydrocolloids, 41*, 53–59. http://dx.doi.org/10.1016/j.foodhyd.2014.03.019.

Farahnaky, A., Dadfar, S. M. M., & Shahbazi, M. (2014). Physical and mechanical properties of gelatin–clay nanocomposite. *Journal of Food Engineering, 122*, 78–83. http://dx.doi.org/10.1016/j.jfoodeng.2013.06.016.

García, N., Hoyos, M., Guzmán, J., & Tiemblo, P. (2009). Comparing the effect of nanofillers as thermal stabilizers in low density polyethylene. *Polymer Degradation and Stability, 94*(1), 39–48. http://dx.doi.org/10.1016/j.polymdegradstab.2008.10.011.

Golebiewski, J., Rozanski, A., Dzwonkowski, J., & Galeski, A. (2008). Low density polyethylene–montmorillonite nanocomposites for film blowing. *European Polymer Journal, 44*(2), 270–286. http://dx.doi.org/10.1016/j.eurpolymj.2007.11.002.

Hemati, F., & Garmabi, H. (2011). Compatibilised LDPE/LLDPE/nanoclay nanocomposites: I. Structural, mechanical, and thermal properties. *The Canadian Journal of Chemical Engineering, 89*(1), 187–196. http://dx.doi.org/10.1002/cjce.20377.

Hotta, S., & Paul, D. R. (2004). Nanocomposites formed from linear low density polyethylene and organoclays. *Polymer, 45*(22), 7639–7654. http://dx.doi.org/10.1016/j.polymer.2004.08.059.

Kanmani, P., & Rhim, J.-W. (2014). Physical, mechanical and antimicrobial properties of gelatin based active nanocomposite films containing AgNPs and nanoclay. *Food Hydrocolloids, 35*, 644–652. http://dx.doi.org/10.1016/j.foodhyd.2013.08.011.

Kontou, E., & Niaounakis, M. (2006). Thermo-mechanical properties of LLDPE/SiO2 nanocomposites. *Polymer, 47*(4), 1267–1280. http://dx.doi.org/10.1016/j.polymer.2005.12.039.

Krepker, M., Prinz-Setter, O., Shemesh, R., Vaxman, A., Alperstein, D., & Segal, E. (2018). Antimicrobial carvacrol-containing polypropylene films: Composition, structure and function. *Polymer, 10*(79), 1–18. http://dx.doi.org/10.3390/polym10010079.

Kuila, T., Bose, S., Mishra, A. K., Khanra, P., Kim, N. H., & Lee, J. H. (2012). Effect of functionalized graphene on the physical properties of linear low density polyethylene nanocomposites. *Polymer Testing, 31*(1), 31–38. http://dx.doi.org/10.1016/j.polymertesting.2011.09.007.

Lim, G.-O., Jang, S.-A., & Song, K. B. (2010). Physical and antimicrobial properties of *Gelidium corneum*/nano-clay composite film containing grapefruit seed extract or thymol. *Journal of Food Engineering, 98*(4), 415–420. http://dx.doi.org/10.1016/j.jfoodeng.2010.01.021.

López-Mata, M., Ruiz-Cruz, S., Silva-Beltrán, N., Ornelas-Paz, J., Zamudio-Flores, P., & Burruel-Ibarra, S. (2013). Physicochemical, antimicrobial and antioxidant properties of chitosan films incorporated with carvacrol. *Molecules, 18*(11), 13735.

López-Mata, M. A., Ruiz-Cruz, S., de Jesús Ornelas-Paz, J., Del Toro-Sánchez, C. L., Márquez-Ríos, E., Silva-Beltrán, N. P., ... Burruel-Ibarra, S. E. (2017). Mechanical, barrier and antioxidant properties of chitosan films incorporating cinnamaldehyde. *Journal of Polymers and the Environment,* 1–10. http://dx.doi.org/10.1007/s10924-017-0961-1.

Memiş, S., Tornuk, F., Bozkurt, F., & Durak, M. Z. (2017). Production and characterization of a new biodegradable fenugreek seed gum based active nanocomposite film reinforced with nanoclays. *International Journal of Biological Macromolecules, 103*, 669–675. http://dx.doi.org/10.1016/j.ijbiomac.2017.05.090.

Mihindukulasuriya, S. D. F., & Lim, L. T. (2014). Nanotechnology development in food packaging: A review. *Trends in Food Science & Technology, 40*(2), 149–167. http://dx.doi.org/10.1016/j.tifs.2014.09.009.

Morawiec, J., Pawlak, A., Slouf, M., Galeski, A., Piorkowska, E., & Krasnikowa, N. (2005). Preparation and properties of compatibilized LDPE/organo-modified montmorillonite nanocomposites. *European Polymer Journal, 41*(5), 1115–1122. http://dx.doi.org/10.1016/j.eurpolymj.2004.11.011.

Morlat-Therias, S., Fanton, E., Gardette, J.-L., Dintcheva, N. T., La Mantia, F. P., & Malatesta, V. (2008). Photochemical stabilization of linear low-density polyethylene/clay nanocomposites: Towards durable nanocomposites. *Polymer Degradation and Stability, 93*(10), 1776–1780. http://dx.doi.org/10.1016/j.polymdegradstab.2008.07.031.

Müller, C. M. O., Laurindo, J. B., & Yamashita, F. (2011). Effect of nanoclay incorporation method on mechanical and water vapor barrier properties of starch-based films. *Industrial Crops and Products, 33*(3), 605–610. http://dx.doi.org/10.1016/j.indcrop.2010.12.021.

Nielsen, L. E. (1967). Models for the permeability of filled polymer systems. *Journal of Macromolecular Science: Part A - Chemistry, 1*(5), 929–942. http://dx.doi.org/10.1080/10601326708053745.

Park, H.-M., Li, X., Jin, C.-Z., Park, C.-Y., Cho, W.-J., & Ha, C.-S. (2002). Preparation and properties of biodegradable thermoplastic starch/clay hybrids. *Macromolecular Materials and Engineering, 287*(8), 553–558. http://dx.doi.org/10.1002/1439-2054(20020801)287:8<553::AID-MAME553>3.0.CO;2-3.

Pereira de Abreu, D. A., Paseiro Losada, P., Angulo, I., & Cruz, J. M. (2007). Development of new polyolefin films with nanoclays for application in food packaging. *European Polymer Journal, 43*(6), 2229–2243. http://dx.doi.org/10.1016/j.eurpolymj.2007.01.021.

Persico, P., Ambrogi, V., Carfagna, C., Cerruti, P., Ferrocino, I., & Mauriello, G. (2009). Nanocomposite polymer films containing carvacrol for antimicrobial active packaging. *Polymer Engineering & Science, 49*(7), 1447–1455. http://dx.doi.org/10.1002/pen.21191.

Ramos, M., Jiménez, A., Peltzer, M., & Garrigós, M. C. (2014). Development of novel nano-biocomposite antioxidant films based on poly (lactic acid) and thymol for active packaging. *Food Chemistry, 162*, 149–155. http://dx.doi.org/10.1016/j.foodchem.2014.04.026.

Rhim, J.-W. (2011). Effect of clay contents on mechanical and water vapor barrier

properties of agar-based nanocomposite films. *Carbohydrate Polymers, 86*(2), 691–699. http://dx.doi.org/10.1016/j.carbpol.2011.05.010.

Rhim, J.-W., Hong, S.-I., Park, H.-M., & Ng, P. K. W. (2006). Preparation and characterization of chitosan-based nanocomposite films with antimicrobial activity. *Journal of Agricultural and Food Chemistry, 54*(16), 5814–5822. http://dx.doi.org/10.1021/jf060658h.

Sanchez-Garcia, M. D., Ocio, M. J., Gimenez, E., & Lagaron, J. M. (2008). Novel polycaprolactone nanocomposites containing thymol of interest in antimicrobial film and coating applications. *Journal of Plastic Film & Sheeting, 24*(3–4), 239–251. http://dx.doi.org/10.1177/8756087908101539.

Ščetar, M., Siročić, A. P., Hrnjak-Murgić, Z., & Galić, K. (2013). Preparation and properties of low density polyethylene film modified by zeolite and nanoclay. *Polymer-Plastics Technology and Engineering, 52*(15), 1611–1620. http://dx.doi.org/10.1080/03602559.2013.828234.

Shah, R. K., Krishnaswamy, R. K., Takahashi, S., & Paul, D. R. (2006). Blown films of nanocomposites prepared from low density polyethylene and a sodium ionomer of poly(ethylene-co-methacrylic acid). *Polymer, 47*(17), 6187–6201. http://dx.doi.org/10.1016/j.polymer.2006.06.051.

Shemesh, R., Krepker, M., Goldman, D., Danin-Poleg, Y., Kashi, Y., Nitzan, N., ... Segal, E. (2015). Antibacterial and antifungal LDPE films for active packaging. *Polymers for Advanced Technologies, 26*(1), 110–116. http://dx.doi.org/10.1002/pat.3434.

Siripatrawan, U., & Harte, B. R. (2010). Physical properties and antioxidant activity of an active film from chitosan incorporated with green tea extract. *Food Hydrocolloids, 24*(8), 770–775. http://dx.doi.org/10.1016/j.foodhyd.2010.04.003.

Sothornvit, R., Rhim, J.-W., & Hong, S.-I. (2009). Effect of nano-clay type on the physical and antimicrobial properties of whey protein isolate/clay composite films. *Journal of Food Engineering, 91*(3), 468–473. http://dx.doi.org/10.1016/j.jfoodeng.2008.09.026.

Suppakul, P. (2012). Alternative technique for the quantitative determination of antimicrobial activity of antimicrobial packaging film containing lipophilic materials. In M. G. Kontominas (Ed.). *Food packaging: Procedures, management and trends*. USA: Nova Science Publishers.

Suppakul, P., Miltz, J., Sonneveld, K., & Bigger, S. W. (2006). Characterization of antimicrobial films containing basil extracts. *Packaging Technology and Science, 19*(5), 259–268. http://dx.doi.org/10.1002/pts.729.

Tornuk, F., Hancer, M., Sagdic, O., & Yetim, H. (2015). LLDPE based food packaging incorporated with nanoclays grafted with bioactive compounds to extend shelf life of some meat products. *LWT - Food Science and Technology, 64*(2), 540–546. http://dx.doi.org/10.1016/j.lwt.2015.06.030.

Zan, L., Fa, W., & Wang, S. (2006). Novel photodegradable low-density polyethylene − TiO_2 nanocomposite film. *Environmental Science & Technology, 40*(5), 1681–1685. http://dx.doi.org/10.1021/es051173x.

Zivanovic, S., Li, J., Davidson, P. M., & Kit, K. (2007). Physical, mechanical, and antibacterial properties of chitosan/PEO blend films. *Biomacromolecules, 8*(5), 1505–1510. http://dx.doi.org/10.1021/bm061140p.